Single-Crystal EPR Spectra of Copper–Manganese Bimetallic Ferrimagnetic Chains

Dante Gatteschi,[*,1a] Olivier Guillou,[1a] Claudia Zanchini,[1a] Roberta Sessoli,[1a] Olivier Kahn,[*,1b] Michel Verdaguer,[1b] and Yu Pei[1b]

Single-crystal EPR spectra of heterobimetallic chain compounds having formulas MnCu(pba)(H$_2$O)$_3$·2H$_2$O (I) and MnCu-(pbaOH)(H$_2$O)$_3$ (II) (pba = 1,3-propanediylbis(oxamato); pbaOH = 2-hydroxy-1,3-propanediylbis(oxamato)) have been recorded in the 300–4.2 K temperature range. The angular dependence of the line widths was discussed in relation to dipolar interactions between the paramagnetic centers, and the dipolar second moments were calculated, confirming the enhancement of the secular terms due to spin-diffusion effects. The anisotropic shifts in the resonance fields observed at low temperature must be due to short-range order effects. These EPR data allow proposal of the spin distributions in both compounds.

Introduction

EPR is a valuable tool for the investigation of low-dimensional magnetic materials. As pointed out by numerous literature reports, it can provide first-hand information on spin dynamics and on the interactions that eventually lead to three-dimensional order.[2–7] The early applications have been mainly on well-behaved systems, possessing relatively high symmetry,[8–12] but an increasing number of reports have appeared in the literature about novel one-dimensional molecular systems, which, although of relatively low symmetry, appear to be useful testing grounds for the theories so far developed for spin dynamics in low dimension.[13–15] Among these novel one-dimensional magnetic systems, the most original are probably those in which two different magnetic centers alternate along the chain axis.[16–18]

The EPR spectra of Cu(hfac)$_2$(NITMe) (hfac = hexafluoro-acetylacetonate; NITMe = 2,4,4,5,5-pentamethyl-4,5-dihydro-1*H*-imidazolyl-1-oxyl 3-oxide), a ferromagnetic linear chain, show an angular dependence of the line width of the type (3 cos^2 θ – 1)^n, as expected for low-dimensional materials, as well as sizable *g* shifts at low temperature, determined by short-range order effects.[13] Mn(hfac)$_2$(NITR) complexes (R = methyl, ethyl, isopropyl, etc.) form ferrimagnetic chains, which also show sizable spin-diffusion effects in the room-temperature EPR spectra.[14,15]

Recently, some of us reported examples of regular linear ferrimagnetic chains, which order either ferro- or antiferromagnetically.[19,20] The compounds have formulas MnCu-

(pba)(H$_2$O)$_3$·2H$_2$O (I) and MnCu(pbaOH)(H$_2$O)$_3$ (II), where pba is 1,3-propanediylbis(oxamato) and pbaOH is the 2-hydroxy derivative.

We report here the single-crystal EPR spectra of both compounds in the temperature range 4.2–300 K.

Experimental Section

The compounds were prepared with the procedure previously described.[19,20] Single-crystal EPR spectra were recorded at X-band frequency with a Bruker ER200 spectrometer and at Q-band frequency with a VARIAN E9 spectrometer. In the X-band experiment the crystals were rotated by means of a goniometer and a quartz rod, while at Q-band frequency the magnet was rotated. Low-temperature spectra were recorded with an Oxford Instruments ESR9 continuous-flow cryostat.

Results

The room-temperature single-crystal EPR spectra of I have been recorded at both X- and Q-band frequencies, with the static magnetic field in the *bc*, *ac*, and *ab* planes of the orthorhombic lattice. The resonance field of the main line is practically independent of the angle, with *g* very close to 2. The line width, on the other hand, is largely angular dependent, as shown in Figure 1. The maxima of ΔB_{pp} are observed along the crystal axes, the order being $\Delta B_c > \Delta B_b > \Delta B_a$. The minima, on the other hand, are observed almost exactly between the maxima at about ±45°. The line widths are within error frequency independent.

In some angular settings a transition at half-field is clearly observed only at X-band frequency. The intensity depends dramatically on the angular setting, and the line width is similar to that of the transition with $\Delta M_S = \pm 1$.

The temperature dependence of the spectra was followed along the three crystal axes. The most notable effect observed is the shift of the resonance fields at temperatures below 30 K, as shown in Figure 2. The shift is upfield parallel to *b*, downfield parallel to *c*, and much less marked parallel to *a*.

The line shape is to a good approximation Lorentzian. Deviations are observed only in the wings, where experimental error is relatively large.

The spectra of II are rather similar to those of I, showing an angular dependence of the line width with $\Delta B_c > \Delta B_b \approx \Delta B_a$, as shown in Figure 3. The minima are observed when the static magnetic field makes an angle of about 45° with the crystal axes in the *ab* and *ac* planes, while in the *bc* plane the minimum is observed close to the magic angle from *c*. No half-field transition was observed for II. The line shapes are Lorentzian to a good approximation.

Also, the spectra of II show a temperature-dependent *g* shift, as shown in Figure 4: the shift is upfield parallel to *a* and *b*, and downfield parallel to *c*.

Discussion

In the EPR spectra of magnetically concentrated systems, the observed line width is the resultant of dipolar interactions, which broaden the lines, and exchange interactions, which narrow the lines. In three-dimensional systems quite often exchange effects

(1) (a) Università di Firenze. (b) Université de Paris-Sud.
(2) Kokoszka, G. F. In *ESR of Low Dimensional Systems: Low Dimensional Cooperative Phenomena*; Keller, K. J., Ed.; Plenum Press: New York, 1975; p 171.
(3) Willett, R. D.; Gaura, R. M.; Landee, C. P. In *Extended Linear Chain Compounds*; Miller, J. S., Ed.; Plenum Press: New York, 1983; Vol. 3, p 143.
(4) Richards, P. M. In *Local Properties at Phase Transitions*; Muller, K. A., Ed.; North-Holland: Amsterdam, 1975; p 539.
(5) Richards, P. M. In *Low Dimensional Cooperative Phenomena*; Keller, H. J., Ed.; Plenum Press: New York, 1975.
(6) Lagendijk, A. *Phys. Rev. B* **1978**, *18*, 1322.
(7) Drumheller, J. E. *Magn. Reson. Rev.* **1982**, *7*, 123.
(8) Lagendijk, A.; De Raedt, H. *Phys. Rev. B* **1977**, *16*, 16.
(9) Okuda, K.; Hata, H.; Date, M. *J. Phys. Soc. Jpn.* **1972**, *33*, 1574.
(10) Ikebe, M.; Date, M. *J. Phys. Soc. Jpn.* **1971**, *30*, 93.
(11) Hughes, R. C.; Morosin, B.; Richards, P. M.; Duffy, W., Jr. *Phys. Rev. B* **1975**, *11*, 1795.
(12) Poertadji, S.; Ablart, G.; Pescia, J.; Clement, S.; Cheik-Rouhou, A. *J. Phys. Lett.* **1983**, *44*, L-561.
(13) Caneschi, A.; Gatteschi, D.; Zanchini, C.; Rey, P. *J. Chem. Soc., Faraday Trans. 1* **1987**, *83*, 3603.
(14) Caneschi, A.; Gatteschi, D.; Laugier, J.; Pardi, L.; Rey, P.; Zanchini, C. *Inorg. Chem.*, in press.
(15) Caneschi, A.; Gatteschi, D.; Rey, P.; Sessoli, R. *Inorg. Chem.*, in press.
(16) Landee, C. P. In *Organic and Inorganic Low Dimensional Crystalline Materials*; Delhaes, P., Drillon, M., Eds.; Plenum Press: New York, 1987; pp 75–92.
(17) Kahn, O. In *Organic and Inorganic Low Dimensional Crystalline Materials*; Delhaes, P., Drillon, M., Eds.; Plenum Press: New York, 1987; pp 93–108.
(18) Benelli, C.; Caneschi, A.; Gatteschi, D.; Rey, P. In *Organic and Inorganic Low Dimensional Crystalline Materials*; Delhaes, P., Drillon, M., Eds.; Plenum Press: New York, 1987; pp 109–124.
(19) Pei, Y.; Verdaguer, M.; Kahn, O.; Sletten, J.; Renard, J. P. *Inorg. Chem.* **1987**, *26*, 138.
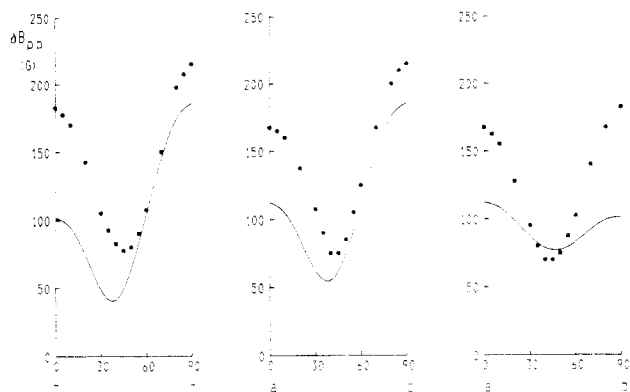(20) Kahn, O.; Pei, Y.; Verdaguer, M.; Renard, J. P.; Sletten, J. *J. Am. Chem. Soc.* **1988**, *110*, 782.

Figure 1. Angular dependence of the ΔB_{pp} line widths of I in the three orthogonal planes *bc*, *ca*, and *ab*. The solid lines represent the calculated values (see text).

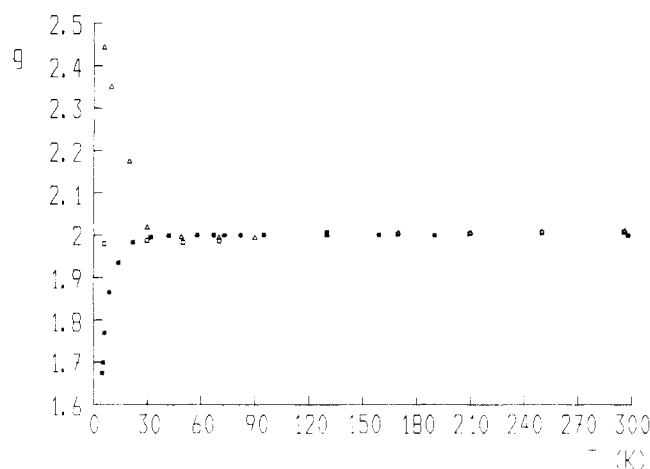**Figure 2.** Temperature dependence of the *g* values for the $\Delta M = \pm 1$ line for I along the *a* (□), *b* (✱), and *c* (△) axes.
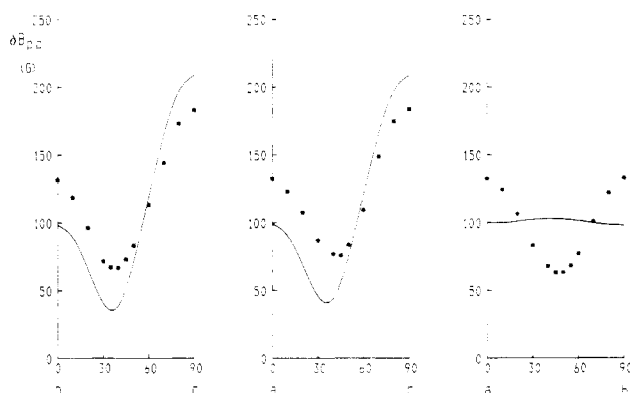

Figure 3. Angular dependence of the ΔB_{pp} line widths of II in the three orthogonal planes *bc*, *ca*, and *ab*. The solid lines represent the calculated values (see text).

dominate, and the lines are exchange narrowed. In one-dimensional systems exchange is much less effective, and the line widths are intermediate between the exchange-narrowed and dipolar-broadened limits.

The reason for this difference is that in one-dimensional systems the movement of a spin deviation is much slower than in a three-dimensional lattice because the number of alternative paths for a disturbance to move from one site to another is much more limited in the former.[21] Therefore, the spectra of one-dimensional systems are mostly affected by the long-time part of the spin correlation function, which is dominated by diffusion (spin-diffusion effects).
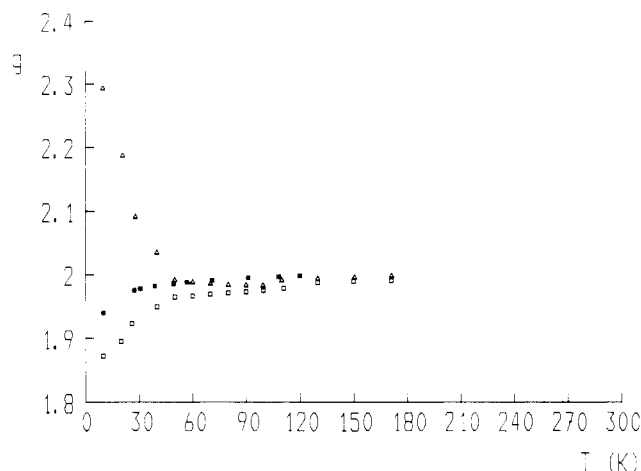
(21) Bencini, A.; Gatteschi, D. In *EPR of Exchange Coupled Systems*; Springer Verlag: Berlin; in press.

Figure 4. Temperature dependence of the *g* values for the $\Delta M = \pm 1$ line for II along the *a* (□), *b* (✱), and *c* (△) axes.

The broad lines observed at room temperature for both I and II are a clear indication of the fact that the exchange-narrowing condition is not obtained, and a confirmation of this comes from the observation of the $\Delta M_S = 2$ transition for I. This behavior must be related to spin-diffusion effects along the chain, although the EPR spectra are not typically one-dimensional. Indeed the principal requisites for a typical one-dimensional behavior are the following: (i) there is a $(3 \cos^2 \theta - 1)^{4/3}$ angular dependence of the line width; (ii) the line shape can be described by the Fourier transform of $\exp(-t^{3/2})$ at $\theta = 0°$ and by a Lorentzian curve at the magic angle; (iii) the magic angle line width is proportional to the inverse square root of the microwave frequency; (iv) a half-field transition is observed. All these properties together are rarely met, but in the present case only the fourth is observed, at least for I. The half-field transition, however, is obviously not typical of one-dimensional magnetic compounds.

The departure of the EPR spectra of these compounds from ideal one-dimensional behavior is easily understood by looking at the structure. In fact, they definitely possess a chain structure,[19,20] and as far as exchange is concerned, they behave as one-dimensional systems, but the strongest dipolar interactions are between the chains, as shown by the short interchain contacts.

Considering that the spins are localized on the copper and manganese ions, respectively, we can estimate the broadening effect on the EPR lines of the dipolar coupling by evaluating the second moment relative to the Mn–Mn, Mn–Cu, and Cu–Cu interactions, with the Kubo–Tomita formalism.[22] The second moments depend on a geometrical factor, which depends on the angle between the static magnetic field and the vector connecting the two interacting spins, on the inverse sixth power of the spin–spin distance, and on a factor determined by the spin quantum numbers.[7,23,24] For identical spins this is given by

$$M_2 = (3/4)S(S + 1)\mu_B^2 g^2 \sum_j r_{ij}^{-6}\{(3 \cos^2 \theta_{ij} - 1) +$$

$$\sin^4 \theta_{ij} \exp[-(1/2)(2\omega_0/\omega_e)^2] +$$

$$10 \cos^2 \theta_{ij} \sin^2 \theta_{ij} \exp[-(1/2)(\omega_0/\omega_e)^2]\} \quad (1)$$

where ω_0 and ω_e are the Zeeman and exchange frequencies respectively, and θ_{ij} and r_{ij} are respectively the angle formed by the direction of the static magnetic field with the vector connecting the two dipolar interacting centers i and j and the distance between them. The first term in the braces is the secular component, while the other two are the nonsecular components. The former is expected to dominate in one-dimensional systems, while all the terms should be used in three-dimensional systems. In the present case the relative importance of the latter terms for the three different types of dipolar interactions is given by the ratio $S_{Mn}(S_{Mn}$

(22) Kubo, R.; Tomita, K. *J. Phys. Soc. Jpn.* **1954**, *9*, 888.
(23) Hennessy, M. J.; McElwee, C. D.; Richards, P. M. *Phys. Rev. B* **1973**, *7*, 930.
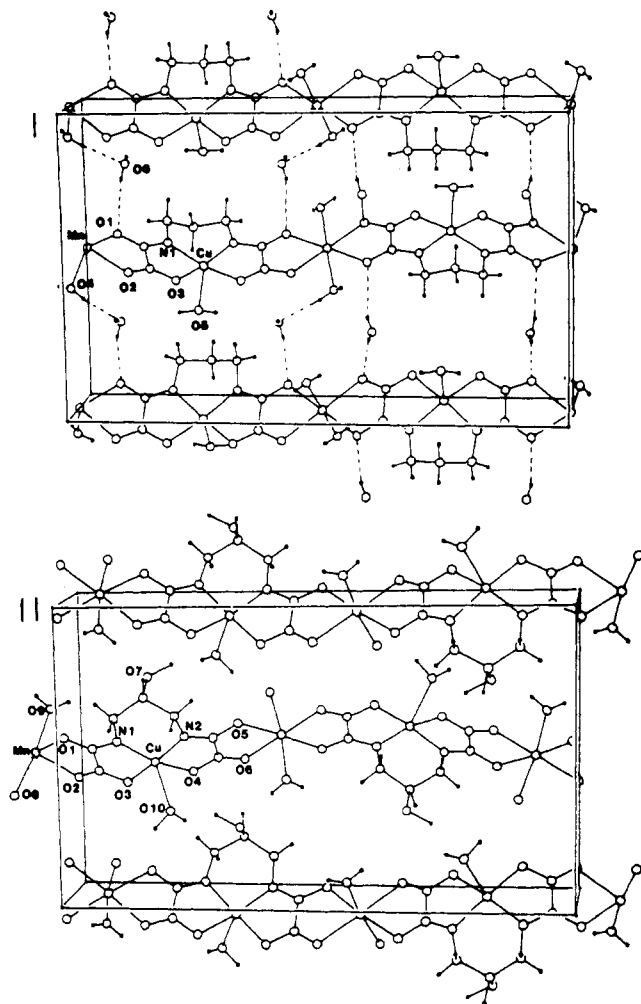(24) McGregor, K. T.; Soos, Z. G. *J. Chem. Phys.* **1976**, *64*, 2506.

Figure 5. Perspective views of the contents of the unit cells of I and II. The *b* axis is the chain axis, and *a* points to the top of the page.

+ 1): $\{2S_{Cu}(S_{Cu} + 1)S_{Mn}(S_{Mn} + 1)/[S_{Cu}(S_{Cu} + 1) + S_{Mn}(S_{Mn} + 1)]\}$: $S_{Cu}(S_{Cu} + 1) = 11.67:1.84:1$, which shows that for similar values of the geometric factors the Mn–Mn interactions will be dominant.

In Figure 5 perspective views of the contents of the unit cells of I and II are given. The two structures[19,20] are fairly similar to each other, with two inequivalent chains present in the unit cell. The *z* molecular axes of the metal ions in the two chains are defined by the perpendiculars to the oxamato planes and make an angle of ca. 90° with each other. The chains in both cases are parallel to the *b* axis. The nearest-neighbor distances within a chain are Cu–Mn, 541.2 (1) pm for I and 537.9 (1) and 543.3 (1) pm for II, while the interchain shortest contacts are between homologous metal ions. The shortest distances are either Mn–Mn or Cu–Cu, 521.1 (1) pm for I and 507.3 (1) pm for II. The manganese ions have four further manganese ions at 697.2 (1) pm for I, while for II there are two manganese ions at 692.2 (1) pm and two others at 817.4 (1) pm. The copper ions have two copper ions at 654.5 (1) pm for I and 711.9 (1) pm for II and two at 773.6 (1) pm for I and 822.8 (1) pm for II.

The largest difference between I and II concerns the shortest metal–metal separations between neighboring chains in the *a* direction. These are Cu--Cu = 654.5 (1) pm and Mn--Mn = 697.7 (1) pm in I and Cu--Mn = 575.1 (1) and 639.8 (1) pm in II. In II, as compared to I, every other chain is displaced by slightly less than half a repeat unit along *b* (see Figure 5).[20] This difference has been considered to be responsible of the fact that I orders antiferromagnetically and II ferromagnetically.

We calculated first the secular dipolar second moment on the basis of the hypothesis that the Mn–Mn contributions are dominant. All the centers that are less than 1500 pm from the central metal ion were included in the calculation, and for II, the sum

was repeated for the two different manganese centers present in the cell. In order to improve the fit we also added Cu–Mn contributions: the corrections were in the right direction, but small. The calculated values are scaled by using the relation[23]

$$\Delta B_{pp} = (4/3)^{2/3} M_2^{2/3}/J^{1/3} \qquad (2)$$

which is expected to be valid for one-dimensional systems. The value of the intrachain Mn–Cu exchange parameter, *J*, was obtained by fitting the magnetic susceptibilities.[19,20] The calculated values are qualitatively in agreement with the experiment, as shown by the solid lines in Figures 1 and 3 for I and II, respectively. In fact, they predict that the largest lines much be observed parallel to *c*, in accord with experiment, with additional maxima parallel to *a* and *b* and minima in the *ac* and *bc* planes. The agreement is less satisfactory in the order of the maxima along *a* and *b*, which is reversed compared to experiment, and also in the angular dependence in the *ab* plane. However, it must be stressed that, given the simplified approach we have used, the results can be considered as satisfactory. Further, they nicely confirm the importance of spin-diffusion effects in these materials. Indeed, if the normal exchange conditions were attained, the angular dependence of the line widths would be different, being determined by the full second moment, rather than by the secular part only, and the line widths would be much smaller since they would be governed by the relation[4]

$$\Delta B_{pp} = M_2/J \qquad (3)$$

From (2) the maximum line widths are calculated as 4.6 G for I and 5.2 G for II, considering only the main Mn–Mn interaction.

Other mechanisms may be responsible for the broadening of the lines of these materials, namely *g* and *A* anisotropies,[25,26] anisotropic exchange,[24] and manganese zero-field splitting. *g* anisotropy apparently is not relevant here because the lines are practically frequency independent and can be safely neglected. *A* anisotropy might be important for the copper ions, but since its contribution is scaled by the small S_{Cu} value, its role should be marginal. Similar considerations can be made for anisotropic exchange, which has been found to be fairly small in copper–manganese pairs.[27] The only term that must be taken into consideration is given by the manganese zero-field splitting. In fact, in the assumption of an axial tensor the second moment has a contribution proportional to $(2S_{Mn} - 1)(2S_{Mn} + 3)D_{Mn}^2/5$. Unfortunately, nothing is known independently about its value; therefore, we must use it as a parameter, but the comparison with the values reported in the literature for manganese(II) complexes shows that *D* can be as large as 0.1 cm^{-1} in distorted octahedral environments. Therefore, we included this term as well in the calculation of the second moment, but we observed only a very small improvement in the fit with respect to that obtained without including manganese zero-field splitting. Additional complications, including nonaxial zero-field splitting, were not included, because the number of parameters would be too large.

Concluding this section, we may state that the simple Kubo–Tomita theory reproduces satisfactorily some of the main features of the angular dependence of the line widths of both I and II, although the details would require a more sophisticated model that at the moment is not available for compounds of low symmetry.

The anisotropic shifts in the resonance fields observed at low temperature (see Figures 2 and 4) are most likely due to short-range order effects, i.e., to the spin correlation length, which is increasing on decreasing temperature. Similar effects were observed in the archetypal one-dimensional compound $[(CH_3)_4]$-$MnCl_3$ (TMMC) and in various other systems.[28–30]

(25) Kumano, M.; Ikegami, Y. *Chem. Phys. Lett.* **1978**, *54*, 109.
(26) Hughes, R. C.; Morosin, B.; Richards, P. M. *Phys. Rev. B* **1975**, *11*, 1795.
(27) Paulson, J. A.; Krost, D. A.; McPherson, G. L.; Rogers, R. D.; Atwood, J. L. *Inorg. Chem.* **1980**, *19*, 2519.
(28) Hoogerbeets, R.; Van Duyneveldt, A. J. *Physica* **1973**, *121*, 233.
(29) Tuchendler, J.; Magarino, J.; Renard, J. P. *Phys. Rev. B* **1979**, *20*, 2637.
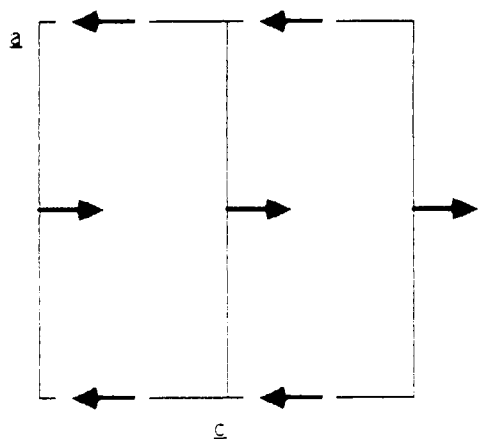(30) Nagata, K.; Tazuke, Y. *J. Phys. Soc. Jpn.* **1972**, *32*, 337.

Figure 6. Schematic representation of the preferred spin orientation for I in the *ac* plane. The arrows indicate the manganese spins; those of the copper ions would be in the opposite directions.

Alternative explanations, which attribute the shifts to intrinsic *g* variations due to selective thermal population of different spin states, do not appear to be relevant here, because in no way could they give both positive and negative deviations from the high-temperature value.

The resonance fields along the three principal axes can be expressed as[28]

$$B_a = \left(\sqrt{\chi_b \chi_c} \middle/ \chi_a\right)(g_e/g_a)B_0 \qquad (4)$$

where χ_a, χ_b, and χ_c are the principal susceptibilities in the paramagnetic region, g_a is the indicated principal *g* value, $g_e = 2.0023$, and B_0 is the resonance field of the free electron. The

resonance fields for the other crystal directions follow from cyclic permutations.

The observed shifts compare well with the reported magnetic anisotropy data, which showed that $\chi_c > \chi_a > \chi_b$ for I and $\chi_c > \chi_a > \chi_b$ for II. The high value observed for χ_c has been attributed to anisotropic exchange that tends to align the spins orthogonal to *a*. The present EPR data at high temperature suggest that the main dipolar interaction must be parallel to *c*, and if we assume that it dominates the interchain interaction, we must conclude that the spins are parallel to each other along this direction. Therefore, an alternative spin distribution for I may be suggested, as compared to ref 19, where the spins were assumed to be oriented by an interchain antiferromagnetic exchange interaction. The suggested spin alignment is shown in Figure 6. Such a spin structure agrees with the weak ferromagnetism observed[20] for I along *a* because the antiferromagnetically coupled manganese(II) ions occupy magnetically nonequivalent sites. In this particular case, where the manganese ion lies in a special position, only canting in the *ac* plane is possible, yielding weak ferromagnetism along *a*. The suggested structure seems to be the only one compatible with magnetic symmetry requirements.[31] The difference between I and II lies mainly in the coupling in the planes orthogonal to *c*: for I this yields alternate planes with antiparallel spin alignment, while for II all the spins are parallel. The nearest-neighbor interactions along *c* are parallel in both cases.

(31) Opechowsky, W.; Guccione, R. In *Magnetism*; Rado, G. T., Suhl, H., Eds.; Academic Press: New York, 1963.

Contribution from the Chemistry Department,
University of Virginia, Charlottesville, Virginia 22901

Matrix Infrared Spectra of Reaction and Photolysis Products of Stibine and Ozone

Lester Andrews,* Brian W. Moores,[1] and Kathleen K. Fonda

Argon-diluted samples of stibine and ozone were codeposited at 12 K and examined by infrared spectroscopy. Isotopic substitution (SbH_3, SbD_3, $^{16}O_3$, $^{18}O_3$, $^{16,18}O_3$) provided a basis for identification of the major reaction products as stibylene ozonide, $HSbO_3$, and hydroxystibine, H_2SbOH. Red photolysis produced new bands identified as stibine oxide, H_3SbO, and ultraviolet photolysis destroyed $HSbO_3$, decreased H_3SbO, increased H_2SbOH, and produced weak bands probably due to $HOSbO_2$.

Introduction

As part of a program involving the study of new reactive molecular species trapped in low-temperature matrices, we have recently investigated the infrared spectra of mixtures of ozone in solid argon with the group 15 hydrides ammonia,[2] phosphine,[3,4] and arsine.[5] These studies have identified several new species formed when the mixtures were irradiated with visible or ultraviolet light. In all of these cases, there is evidence for the formation of a stable complex between the precursor ozone and hydride submolecules, and reaction occurs following red photolysis of the molecular complex, which does not photolyze ozone isolated in solid argon. First, the ozone submolecule in the complex undergoes photodissociation, and the photolytically generated oxygen atom then adds to the hydride submolecule within the complex. In the case of phosphine and arsine, a substantial yield of photoproducts was formed when irradiation was carried out by using red light.[4,5] Since the cross section for absorption of 600-nm photons by

isolated ozone molecules is smaller by a factor of 10^5 than that for 250-nm photons,[6] the complex appears to have a much higher probability for red photodissociation than does isolated ozone.

In the ammonia–ozone and phosphine–ozone reactions, no evidence for reaction between the precursor molecules was found during codeposition before photolysis. In the case of arsine and ozone, however, reaction products were formed during codeposition of the samples. We have carried out a study of the stibine–ozone system, motivated by a desire to complete a systematic investigation of the matrix reaction of group 15 hydrides with ozone and to discover possible periodic trends in their reactivity and photochemistry. A further motivation for this work was the relative

(1) On sabbatical leave from Randolph-Macon College, Ashland, VA 23005.
(2) Withnall, R.; Andrews, L. *J. Phys. Chem.* **1988**, *92*, 2155.
(3) Withnall, R.; Hawkins, M.; Andrews, L. *J. Phys. Chem.* **1986**, *90*, 575.
(4) Withnall, R.; Andrews, L. *J. Phys. Chem.* **1987**, *91*, 784.
(5) Andrews, L.; Withnall, R.; Moores, B. W. *J. Phys. Chem.*, in press.
(6) Baulch, D. L.; Coty, R. A.; Crutzen, P. J.; Hampson, R. F.; Kerr, J. A.; Troe, J.; Watson, R. T. *J. Phys. Chem. Ref. Data* **1982**, *11*, 327.

* To whom correspondence should be addressed.